RSC Advances




ROYAL SOCIETY OF CHEMISTRY

www.rsc.org/advances

RSC Advances

RSCPublishing

ARTICLE

# Two-Dimensional Correlation Infrared Spectroscopy Reveals the Detailed Molecular Movements during the Crystallization of Poly(ethylene-co-vinyl alcohol)

Cite this: DOI: 10.1039/xoxxoooooox

Received ooth January 2012,
Accepted ooth January 2012

DOI: 10.1039/xoxxoooooox

www.rsc.org/

Gehong Su,[a] Tao Zhou,[a,*] Xifei Liu,[a] Jihai Zhang,[a] Jianjun Bao,[a,*] and Aiming Zhang[a]

In this paper, the quantitative spectroscopic evidence for the leading role of hydrogen bonds during the cooling crystallization of poly(ethylene-co-vinyl alcohol) (EVOH) was successfully obtained. Furthermore, the detailed molecular movements during the crystallization of EVOH were revealed via two-dimensional correlation infrared spectroscopy. Two cooling crystallization processes were detected at 159 °C and around 101-105 °C via the combination of DSC and the newly proposed scaling-MW2D correlation FTIR spectroscopy. These two crystallization processes were defined as the primary crystallization (region I) and secondary perfection process (region II) of EVOH. The methods of calculating the enthalpies of the pair-bonded hydrogen bonding ($\Delta H_h$), vinyl alcohol (VA) repeating unit crystallization ($\Delta H_{C\text{-}VA}$), VA repeating unit diffusing into the crystal lattice ($\Delta H_{l\text{-}VA}$), and ethylene (ET) repeating unit crystallization ($\Delta H_{C\text{-}ET}$) were established via Van't Hoff plots. For region I and II, the contributions of the pair-bonded hydrogen bonding of VA repeating units to entire EVOH crystallization were 42.8% ($\Delta H_h$=-90.4±5.2 kJ/mol) and 64.6% ($\Delta H_h$=-75.8±3.1 kJ/mol). However, the contributions of the ET crystallization to EVOH crystallization were 19.4% ($\Delta H_{C\text{-}ET}$=-41.0±2.0 kJ/mol) and 32.7% ($\Delta H_{C\text{-}ET}$=-38.3±0.8 kJ/mol), which were only a half of the contribution of pair-bonded hydrogen bonding. The 2D correlation analysis was used to investigate the sequential order of groups' movement involved in the crystallization. It was found that Region I had 3-steps. The first step is the formation of hydrogen bonds of VA repeating unit, and the second step is VA repeating unit diffusing into the crystal lattice, resulting in the primary crystallization. The third step is the ET repeating unit crystallization accompanied by the movement of VA repeating unit without hydrogen bonding in the amorphous. Region II had 4-steps. The first step is also the generation of hydrogen bonds of VA repeating unit. The second step is a local rearrangement of the lattice in the imperfect crystalline of VA repeating unit, called as the secondary perfection process. The third step is the movement of VA repeating unit without hydrogen bonding in the amorphous. The fourth step is the weak crystallization of ET repeating unit at a low temperature.

## 1. Introduction

Poly(ethylene-co-vinyl alcohol) (EVOH) random copolymer is a semicrystalline material with an excellent gas-barrier property that have been widely applied to various industry fields, such as food packaging, plastic container, and gasoline tanks.[1-8] Recently, EVOH have attracted plenty of research passion in fields of water treatment and biomedical science due to its hydrophilicity and good blood compatibility.[9, 10] The EVOH copolymers are commonly synthesized via a saponified reaction from ethylene-co-vinyl acetate copolymer, and the chains of EVOH copolymers are constructed by random sequence of ethylene (ET) and vinyl alcohol (VA) monomeric units.[11, 12] The gas-barrier properties of EVOH are largely dependent upon the content of ethylene segment, normally, the gas-barrier properties decrease with the increasing of the ethylene segment. EVOH copolymer with different comonomer content is easy to crystallize, whose the degree of crystallinity usually reaches 70%, and its properties also change a lot alone with the compositions.[3, 13-16] The EVOH copolymers show an excellent gas-barrier performance due to the formation of a large amount of intra- and intermolecular hydrogen bonds of the hydroxyl groups on VA segments.[3, 17] These hydrogen bonds also strongly enhance the interchain cohesion, and decrease the free volume of EVOH, resulting in the great difficulty of the small gas molecules diffusing through the polymer matrix.[18-21]

In the past few decades, the crystallization behavior of EVOH copolymers has been extensively studied. It was proved that EVOH could form two types of crystals upon cooling from the melts. These crystals include orthorhombic crystalline and monoclinic crystalline when the content of VA comonomer is 0–40 mol.% and 40–60 mol.%, respectively.[13, 14] Cerrada reported that the orthorhombic crystalline was generated for slowly crystallized samples.[15] Lopez-Rubio investigated the influence of cooling rate on the crystalline morphology of EVOH, and the formation of the orthorhombic crystalline was also discovered at a high cooling speed.[16] The orthorhombic crystalline had a tendency to transform into the monoclinic after an annealing treatment.[16] It was reported that both ET and VA segments were incorporated into the crystal lattice during the crystallization process of EVOH, forming a mixed crystal. However, the capacity of ET and VA segments diffusing into the lattice was different.[13-16] The hydrogen bonds generated by the hydroxyl groups of VA segments play an important rule on the various properties of EVOH. Certainly, the crystallization behavior of EVOH is strongly influenced by the hydrogen bonds. However, the role of the hydrogen bonding on the crystallization process of EVOH has been unclear so far. Furthermore, the quantitative evidence for the role of hydrogen bonding during EVOH crystallization still lacks. So, a depth understanding of the hydrogen bonding during the EVOH crystallization will have a great scientific and practical value.

Generalized two-dimensional (2D) correlation infrared spectroscopy was originally proposed by Noda in 1993,[22] which has become a very important spectroscopy method. Due to spreading spectral peaks over the second dimension, the spectral resolution of this method is significantly enhanced compared with 1D FTIR spectra.[23] Thus, the 2D correlation spectra can capture the information which is not obvious or overlapped in the 1D spectra. In addition, the sequential order of spectral variables can be easily obtained from the 2D correlation infrared spectra according to Noda's rules. So, 2D correlation infrared spectroscopy can be conveniently used to investigate the detailed mechanism of material's transitions. In 2000, Thomas and Richardson proposed moving-window two-dimensional correlation spectroscopy (MW2D),[24] which can be used to determine the transition temperature of a thermotropic liquid-crystal sample. MW2D can be directly applied to see the spectral correlation variation along both perturbation variables (e.g., temperature) and spectral variables (e.g., wavenumber) axis. After that, a similar method based on the MW2D was proposed by Morita in 2006, which is called perturbation-correlation moving-window two-dimensional correlation spectroscopy (PCMW2D).[25] Recently, we have proposed the scaling moving-window two-dimensional correlation spectroscopy (scaling-MW2D), which was designed to identify weak transitions of materials.[26] The reason which we established scaling-MW2D is that the conventional MW2D (by Thomas and Richardson) has a difficulty to distinguish the weak transitions because of its low resolving capacity along the perturbation variable axis (e.g. temperature) in MW2D spectra.[26] For scaling-MW2D, the concept of scaling factor α is provided.[26] People can highlight interesting weak transitions by altering this scaling factor.

The 2D correlation infrared spectroscopy has an inherent advantage in the study of polymer transitions, especially the transitions of hydrogen bonds involved in.[27-36] In the past five years, scientists found that the best way of implementation is the combination of 2D correlation infrared spectroscopy with moving-widow and generalized 2D correlation analysis.[32, 37-42] General speaking, MW2D or PCMW2D was first employed to determine the transition point and the transition region of polymers; then, generalized 2D analysis was performed to study the sequential orders of functional groups at a given transition.[32, 37-42] Many successful applications were reported in the study of the mechanism of polymer physical or chemical transitions.

In the present study, two regions of the EVOH crystallization are determined via the combination of differential scanning calorimetry (DSC) and scaling-MW2D correlation FTIR spectroscopy. In addition, the methods of calculating the enthalpies of the pair-bonded hydrogen bonding ($\Delta H_h$), VA repeating unit crystallization ($\Delta H_{C\text{-}VA}$), and ET repeating unit crystallization ($\Delta H_{C\text{-}ET}$) are established via Van't Hoff plots. Also, the relationship of the enthalpies among EVOH crystallization ($\Delta H_{C\text{-}EVOH}$), $\Delta H_{C\text{-}ET}$, $\Delta H_h$, VA repeating unit diffusing into the crystal lattice ($\Delta H_{l\text{-}VA}$) is proposed. So, the contribution of pair-bonded hydrogen bonding to EVOH crystallization can be estimated quantitatively. The powerful 2D correlation analysis is used to investigate the sequential order of groups' movement involved in the crystallization process of EVOH. All the results from this paper confirm that two regions of the EVOH crystallization are both dominated by the pair-bonded hydrogen bonding.

## 2. Experimental

### 2.1. Materials

EVOH was purchased from Nippon Synthetic Chemical Industry Co., Ltd with the ethylene content of 32 mol.% (labeled as EVOHDC3203), and its melt index was 3.2 g/10min (2.16 kg, 190 °C). EVOH used here was designed for large-scale applications for packaging materials (such as packaging films), which has an outstanding processing performance and a gas-barrier property.

### 2.2. Sample preparation

The EVOH film used in FTIR measurement was prepared by heat-pressing. Several EVOH particles of 1 g were first sandwiched between two polyethylene terephthalate (PET) sheets, and then were placed into a hot-press at 200 °C with a pressure of 20 MPa for 20 seconds. After that, the EVOH film samples were air cooled to room temperature. The thickness of prepared film was approximately 10-20 μm. The EVOH film was finally cut into a circular shape (Φ13 mm) by a cutter.

### 2.3. DSC measurement



 

DSC measurements were carried out using DSC 204 F3 (NETZSCH) with about 8 mg EVOH samples in the nitrogen atmosphere (25 ml/min). The samples were initially heated from 30 °C to 225 °C at 20 °C/min, and kept at 225 °C for 3 min to eliminate the thermal history. Subsequently, the samples were cooled down to 40 °C at 5 °C/min, 10 °C/min, and 20 °C/min, respectively. After that, the samples stayed at 40 °C for 3 min, and finally reheated again to 225 °C at 5 °C/min, 10 °C/min, and 20 °C/min.

### 2.4. In situ FTIR spectroscopy

Nicolet iS10 Fourier transform spectrometer equipped with a deuterated triglycine sulfate (DTGS) detector was used for FTIR experiment. Each FTIR spectrum was obtained by 20 scans with a resolution of 4 $cm^{-1}$.The EVOH film prepared before was sandwiched between two KBr windows to prevent the flowing at a high temperature, and then was placed into a home-made in-suit pool (programmable heating and cooling device). EVOH film was firstly heated from 30 °C to 230 °C at 5 °C/min, and then kept at 225 °C for 3 min to eliminate the thermal history. The molten EVOH film was then cooled from 225 °C to 50 °C at 5 °C/min. The temperature-dependent FTIR spectra were collected at cooling process, and there were 119 spectra gathered. During FTIR experiment, the sample was protected by a dried high-purity nitrogen gas (200 ml/min).

### 2.5. Two-Dimensional Correlation Analysis

Scaling-MW2D, MW2D, and generalized 2D correlation FTIR spectra were processed, calculated, and plotted by 2DCS software, developed by one of the authors. The window size of scaling-MW2D and MW2D was chosen as 11 ($2m+1$) to produce high-quality spectra. The linear baseline corrections were applied in the region of 3660−2700 $cm^{-1}$ and 780−700 $cm^{-1}$ before analysis. The 3% correlation intensity of spectra was regarded as noise and was cut off. In 2D correlation FTIR spectra, the pink areas represent positive correlation intensity, and the blue areas represent the negative correlation intensity. The theory and algorithm of MW2D and generalized 2D correlation spectroscopy can refer to the literature.[22-24, 43] Here, a brief introduction to the theory of scaling-MW2D based on auto-correlation is below:

$A(v, I)$ is a $M\times N$ spectral intensity data matrix. $I$ and $v$ are perturbation variable (e.g. temperature) and spectral variable (e.g. wavenumber), respectively.

$$A(v,I)=\begin{pmatrix} y(v,I_1) \\ \vdots \\ y(v,I_j) \\ \vdots \\ y(v,I_M) \end{pmatrix} \quad (1)$$

The reference spectrum and dynamic spectrum in the $j$th submatrix of $A(v, I)$ are calculated according to equation (2) and equation (3).

$$\bar{y}(v)=\frac{1}{2m+1}\sum_{J=j-m}^{j+m} y(v,I_J) \quad (2)$$

$$\tilde{y}(v,I_J)=y(v,I_J)-\bar{y}(v) \quad (3)$$

where $J$ corresponds to the index of rows. A mean-centered $j$th submatrix of $A(v, I)$ is obtained.

$$\tilde{a}_j(v,I)=\begin{pmatrix} \tilde{y}(v,I_{j-m}) \\ \vdots \\ \tilde{y}(v,I_j) \\ \vdots \\ \tilde{y}(v,I_{j+m}) \end{pmatrix} \quad (4)$$

The $\tilde{a}_j(v, I)$ has $2m+1$ rows which is called the window size. The index range of the perturbation variable $I$ of $\tilde{a}_j(v, I)$ is from $j-m$ to $j+m$. Then, the generalized synchronous 2D correlation spectra is calculated from $\tilde{a}_j(v, I)$ according to equation (5).

$$\Phi_j(v_1,v_2)=\frac{1}{2m}\sum_{J=j-m}^{j+m}\tilde{y}(v_1,I_J)\cdot\tilde{y}(v_2,I_J) \quad (5)$$

For each window, the standard deviations of spectral intensities at $v_1$ and $v_2$ are defined in equation (6) and equation (7).

$$\sigma(v_1)=\sqrt{\Phi_j(v_1,v_1)} \quad (6)$$

$$\sigma(v_2)=\sqrt{\Phi_j(v_2,v_2)} \quad (7)$$

The correlation coefficient $\rho(v_1,v_2)$ is defined as follows:

$$\rho(v_1,v_2)=\Phi_j(v_1,v_2)/[\sigma(v_1)\cdot\sigma(v_2)] \quad (8)$$

The scaled forms of the synchronous correlation spectrum in each window are defined:

$$\Phi_j(v_1,v_2)^{(Scaled)}=\Phi_j(v_1,v_2)\cdot[\sigma(v_1)\cdot\sigma(v_2)]^{-\alpha}\cdot\left|\rho(v_1,v_2)\right|^{\beta} \quad (9)$$

The constant α is called as the scaling factor, and β is correlation enhance factor. The value of α is limited to 0−1.0. For scaling-MW2D based on auto-correlation, the each row ($\Omega_{A,j}(v, I_j)$) of the correlation matrix of scaling-MW2D is directly extracted from a diagonal line ($v_1=v_2$) of $\Phi_j^{(Scaled)}$ matrix. The auto-correlation scaling-MW2D correlation spectrum is obtained through sliding window position from $j=1+m$ to $M-m$ and repeating calculations of equation (2)-(9) at each window.

Here, we also provide an easier way to gain an auto-correlation scaling-MW2D spectrum. According to equation (9), the auto-correlation scaling-MW2D can be described as follows.

$$\Phi_j(v_1,v_1)^{(Scaled)}=\Phi_j(v_1,v_1)\cdot[\sigma(v_1)\cdot\sigma(v_1)]^{-\alpha}\cdot\left|\rho(v_1,v_1)\right|^{\beta} \quad (10)$$

$$\rho(v_1,v_1)=\Phi_j(v_1,v_1)/[\sigma(v_1)\cdot\sigma(v_1)]=1 \quad (11)$$

$$\Phi_j(v_1,v_1)^{(Scaled)}=[\Phi_j(v_1,v_1)]^{1-\alpha} \quad (12)$$

A conventional auto-correlation MW2D spectrum is obtained when the value of the scaling factor α=0. In the present study, the value of α=0.618 was chosen according to our previous study. The detailed theory and algorithm of scaling-MW2D can refer to the Ref.[26]

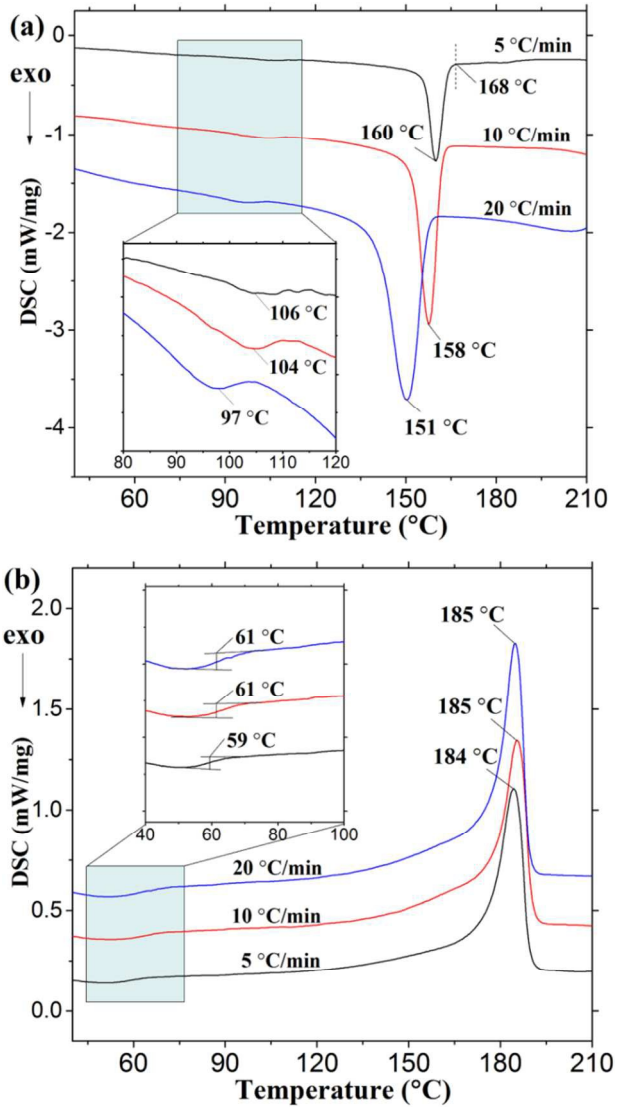


**Figure 1.** DSC curves for EVOH copolymer. **(a)** from 210 °C to 40 °C upon cooling with 5 °C/min, 10 °C/min, and 20 °C/min; **(b)** from 40 °C to 210 °C upon reheating with 5 °C/min, 10 °C/min, and 20 °C/min.

## 3. Results and discussion

### 3.1. DSC measurement

The DSC curves of EVOH at cooling and reheating with 5 °C/min, 10 °C/min, and 20 °C/min are shown in **Figure 1**. In **Figure 1(a)**, the exothermic peaks are observed at 160 °C, 158 °C, and 151 °C when the cooling rates are 5 °C/min, 10 °C/min, and 20 °C/min, respectively, which correspond to the maximum crystallization temperatures of EVOH at different cooling rates. The maximum crystallization temperature decreases with the cooling rate increasing. It also can be observed that weak exothermic peaks appear when the temperature within 80-120 °C (below the maximum crystallization temperature). An enlarged image is also displayed in **Figure 1(a).** These weak exothermic peaks are determined at 106 °C, 104 °C, and 97 °C when the cooling rates are 5 °C/min, 10 °C/min, and 20 °C/min, respectively. However, the peak at 106 °C with 5 °C/min is more difficult to distinguish than the peaks at 104 °C (10 °C/min) and 97 °C (20 °C/min). Although the maximum crystallization temperatures of EVOH can be judged in **Figure 1**, the assignment of weak exothermic peaks at 106 °C, 104 °C, and 97 °C are unclear. **Figure 1(b)** illustrates the DSC curves at reheating. The glass transition of EVOH can be easily determined at 59−61 °C, which shows a typical S-type shape. The melting point of EVOH is observed at 184−185 °C. The temperature of the glass transition of EVOH is obviously lower than that of weak exothermic peaks found in **Figure 1(a)**.

**Table 1.** Band assignments for FTIR spectra of EVOH copolymer

| Wavenumber ($cm^{-1}$) | Assignments | |
|---|---|---|
| | Vinyl alcohol repeating unit (VA) | Ethylene repeating unit (ET) |
| 3490 | $\nu$(O−H, free), O−H stretching of "free" O−H groups | -- |
| 3310 | $\nu$(O−H, bonded), O−H stretching of hydrogen-bonded O−H groups | -- |
| 2932 | $\nu_{as}$(−$CH_2$−), C−H asymmetrical stretching of −$CH_2$−groups | $\nu_{as}$(−$CH_2$−) |
| 2903 | $\nu_s$(−CH−), C−H stretching of −CH−groups | |
| 2854 | $\nu_s$(−$CH_2$−), C−H symmetrical stretching of −$CH_2$−groups | $\nu_s$(−$CH_2$−) |
| 1139 | $\nu_s$(−C−O−, crystals), −C−O− stretching of VA repeating unit in crystals | -- |
| 1100 | $\nu_s$(−C−O−, amorphous), −C−O− stretching of VA repeating unit in amorphous | -- |
| 725 | -- | $\gamma$(−$CH_2$−, crystals), C−H rocking of −$CH_2$−groups of ET repeating unit in crystals |

### 3.2. Temperature-dependent FTIR upon cooling

The temperature-dependent FTIR spectra of EVOH upon cooling from 225 °C to 50 °C in the region 3660−2700 $cm^{-1}$ and 1160−700$cm^{-1}$ are illustrated in **Figure 2**. For clarity, not all the spectra are displayed. The assignments of bands in **Figure 2** and the corresponding explanations are listed in **Table 1**.[32, 44-51] In **Figure 2(a)**, the bands at 3490 $cm^{-1}$ are assigned to O−H stretching of "free" O−H groups in vinyl alcohol repeating units of EVOH, and 3310 $cm^{-1}$ is O−H stretching of hydrogen-bonded O−H groups in VA repeating unit.[44, 45] The bands at 2932 $cm^{-1}$ and 2854 $cm^{-1}$ are attributed to C−H asymmetrical stretching and symmetrical stretching of −$CH_2$−groups in both VA and ET repeating unit, respectively.[45, 46] The bands at 2903 $cm^{-1}$ is assigned to C−H stretching of −CH− groups in VA

repeating unit.[45, 46] It is clearly observed that the bands at 3490 $cm^{-1}$ significantly moves to 3310 $cm^{-1}$ when the temperature decreases from 225 °C to 50 °C. Moreover, the intensity and the width of 3310 $cm^{-1}$ obviously increases and broadens upon cooling. These features indicate the generation of hydrogen bonds in VA repeating unit of EVOH.

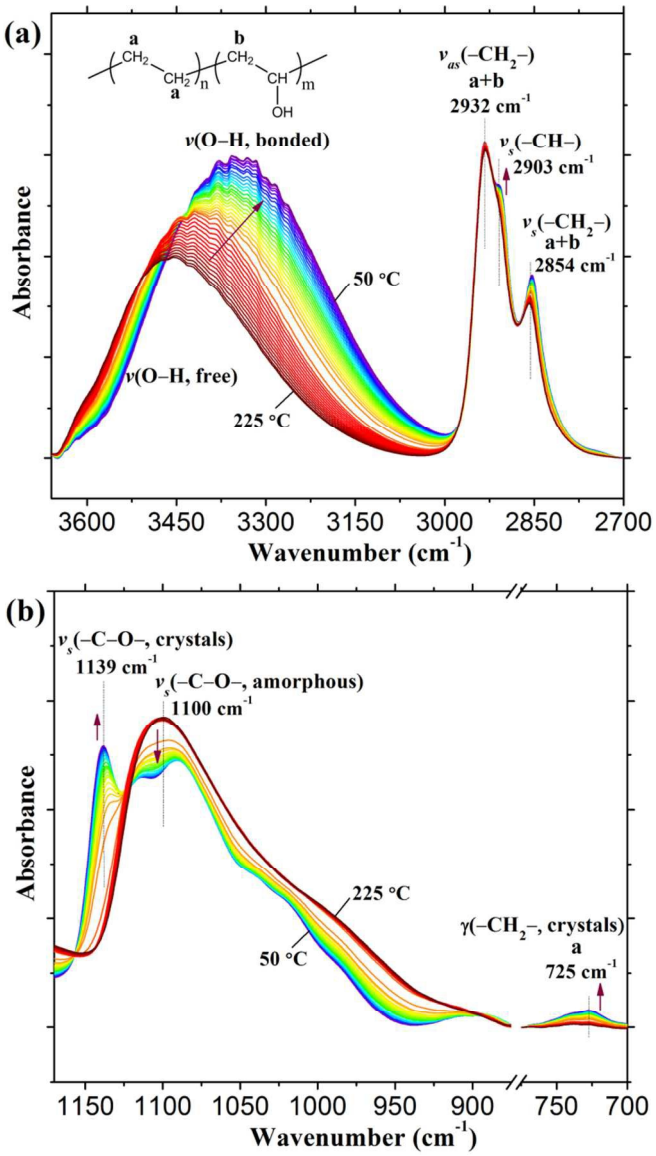


**Figure 2.** The temperature-dependent FTIR spectra of EVOH upon cooling from 225 °C to 50 °C. **(a)** 3660–2700 $cm^{-1}$; **(b)** 1160–700$cm^{-1}$.

In **Figure 2(b)**, the bands at 1139 $cm^{-1}$ and 1100 $cm^{-1}$ are both assigned to −C−O− stretching of VA repeating unit.[32, 45, 47-51] The 1139 $cm^{-1}$ is −C−O− stretching in the crystals, and 1100 $cm^{-1}$ is attributed to −C−O− stretching in the amorphous.[32, 45, 47-51] The bands at 725 $cm^{-1}$ is assigned to C−H rocking of $-CH_2-$groups of ET repeating unit.[45] Here, 1139 $cm^{-1}$ and 725 $cm^{-1}$ are the characteristic bands of the crystalline in VA and ET repeating unit, respectively. The appearance and the intensity increasing of 1139 $cm^{-1}$ reveals the crystallization of VA repeating unit of EVOH when the temperature decreasing from 225 °C to 50 °C. At the same time, the intensity at 1100 $cm^{-1}$ decreases, which represents the process of the amorphous of VA repeating unit transforms into the crystalline. The enhancement of the intensity at 725 $cm^{-1}$ also indicates the formation of the crystals of ET repeating unit upon cooling. The temperature-dependent FTIR spectra of EVOH reveal not only the formation of the crystalline of both VA and ET repeating unit, but also the generation of hydrogen bonds of VA repeating unit upon cooling.

### 3.3. Crystallization regions of EVOH determined by scaling-MW2D FTIR

As shown in **Figure 3**, the conventional MW2D FTIR spectra of EVOH upon cooling in the region 3660−2700 $cm^{-1}$, 1170−950 $cm^{-1}$, and 780−700 $cm^{-1}$ are first calculated. However, due to the great difficulty of detecting weak transitions of polymers,[26] only a transition at 159 °C is determined in the conventional MW2D. This transition is the maximum crystallization temperature of EVOH, which have been observed in DSC curves (**Figure 1**). In the present study, the second derivative of temperature-dependent FTIR spectra in the regions 3660−2700 $cm^{-1}$ and 1160−700$cm^{-1}$ was also calculated according to Savitsky-Golay method, and the Omnic 8.1 software was used. As shown in **Figure S1** in the supporting information, the second derivative is helpful to distinguish the overlapping bands in the original FTIR spectra, and it also has some ability to detect small changes in absorbance in the wavenumber axis. However, such as temperature-dependent FTIR spectra, the second derivative has no capacity to determine the transition point and transition regions in temperature axis, not to mention to detect weak transitions.

The auto-correlation scaling-MW2D was then employed in our work, and the scaling-MW2D FTIR spectra of EVOH in the region 3660−2700 $cm^{-1}$, 1170−950 $cm^{-1}$, and 780−700 $cm^{-1}$ are shown in **Figure 4**. As expected, the scaling-MW2D FTIR spectra detect two transitions at 159 °C and 101−105 °C. The former is the maximum crystallization temperature of EVOH, and the latter corresponds to the weak exothermic peak found in DSC (**Figure 1**). In **Figure 4**, 1139 $cm^{-1}$ and 725 $cm^{-1}$ appear correlation peaks at the transition of 101−105 °C. Because 1139 $cm^{-1}$ and 725 $cm^{-1}$ are the crystalline bands of EVOH, the transition of 101−105 °C is attributed to the secondary perfection process of EVOH. In DSC measurement (**Figure 1**), the weak peaks around 97−106 °C is exothermic, which is also in line with one of the characteristics of crystallization. During the secondary perfection process, the temperature point of 1139 $cm^{-1}$ is at 105 °C, which is 4 °C higher than that of 725 $cm^{-1}$ (101 °C). This reveals that the secondary perfection process of VA repeating unit is before ET repeating unit. In scaling-MW2D FTIR spectra, a large drift of the bands around 3310 $cm^{-1}$ from 3350 $cm^{-1}$ to 3260 $cm^{-1}$can be also observed when the temperature decreases from 216 °C to 60 °C. The crystallization process of EVOH determined by scaling-MW2D is consistent with that of the detected by DSC, and two regions are observed. The first region is the maximum crystallization temperature at 159 °C, and the second region is the secondary

perfection process around 101−105 °C. As shown in **Figure 4**, the temperature regions of these two crystallization processes can also be determined within 170-145 °C (named as region I) and 112-85°C (named as region II), respectively. It should point out that these two processes are both continuous processes, not only occur at the transition temperature. That is to say, the crystallization processes are continuous within region I and region II. The transition points of 159 °C and 101−105 °C are the temperatures, which have a maximum crystallization rate, also correspond to the crystallization peaks observed in DSC curves.

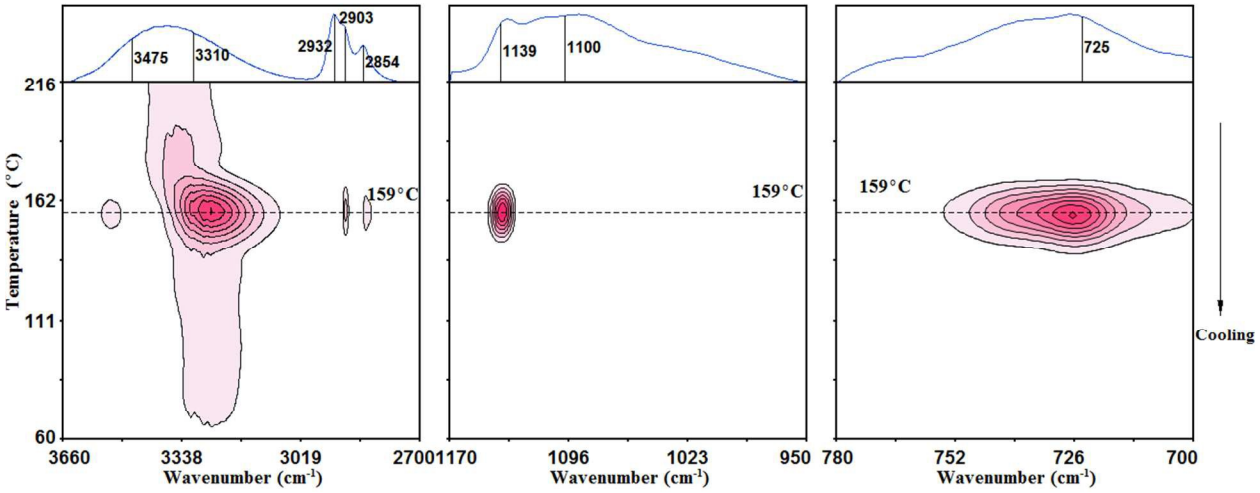


**Figure 3.** Conventional MW2D FTIR spectra of EVOH upon cooling in the region 3660−2700 $cm^{-1}$, 1170−950 $cm^{-1}$, and 780−700 $cm^{-1}$.

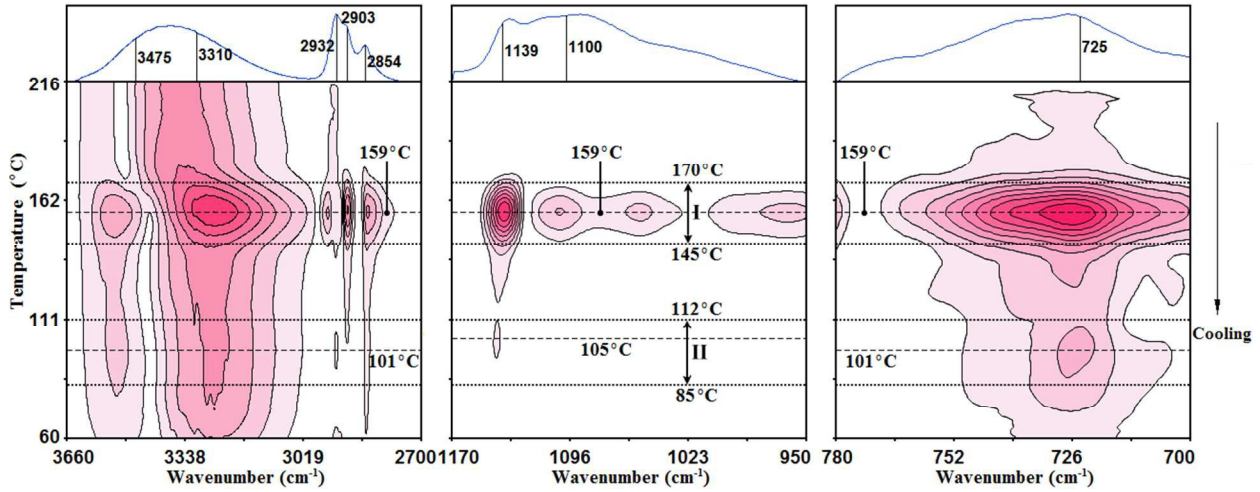


**Figure 4.** Scaling-MW2D FTIR spectra of EVOH upon cooling in the region 3660−2700 $cm^{-1}$, 1170−950 $cm^{-1}$, and 780−700 $cm^{-1}$. The scaling factor is chosen as α=0.618.

The absorbance change extracted from the temperature-dependent FTIR spectra of EVOH at 3310 $cm^{-1}$ and 1139 $cm^{-1}$ from 225 °C to 50 °C upon cooling is illustrated in Figure S2 in the supporting information. For 3310 $cm^{-1}$, it can be clearly observed two sudden changes of absorbance around 159 °C and 103 °C. These two temperatures are very close to the results determined by scaling-MW2D. The sudden change of absorbance around 159 °C is more obvious than that of around 103 °C. The absorbance at 3310 $cm^{-1}$ of both sudden changes is increased upon cooling, which shows the generation of hydrogen bonds in VA repeating unit. For 1139 $cm^{-1}$, a sudden change of absorbance around 159 °C is also observed. The increase of absorbance around 159 °C reveals the crystalline formation of VA repeating unit. However, unlike 3310 $cm^{-1}$, no sudden change can be discerned around 103 °C. This is to say, the secondary perfection process cannot be distinguished from the absorbance change at 1139 $cm^{-1}$. The absorbance change at 725 $cm^{-1}$ upon cooling is also plotted in **Figure S3** in the supporting information.

### 3.4. Enthalpy of the generation of hydrogen bonds and the crystallization estimated from FTIR

The generation and breaking of hydrogen bonds of VA repeating unit (represented by 3310 $cm^{-1}$) can be seen as an equilibrium reaction, considering the hydrogen bonds formation involved in EVOH crystallization is pair-bonded.

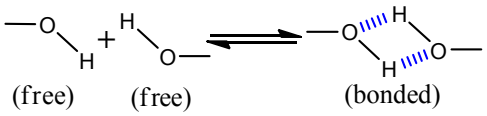


(13)

[H−O] [H−O] [H−O···H−O]
$(1-\alpha_B)C_0$ $(1-\alpha_B)C_0$ $\alpha_B C_0$

where [H−O···H−O] is the molar concentration of pair-bonded hydroxyl groups in VA repeating unit, and [H−O] is the molar concentration of a single free hydroxyl group.

The relationship between absorbance A and the molar concentration C can be expressed as Beer-Lambert Law:[52]

$$A = \varepsilon LC \tag{14}$$

where ε is the extinction coefficient, and L is the optical path of the sample.

At a lower temperature $T_{low}$, the total concentration of the pair-bonded hydroxyl groups is $C_0$. The concentration of the pair-bonded hydroxyl groups and free hydroxyl groups are $C_B$ and $C_F$ at a higher temperature $T_{high}$, respectively. The free hydroxyl groups can be gradually converted to the pair-bonded hydroxyl groups when the temperature decreases. So, the following relationship exists:

$$C_B + C_F = C_0 \tag{15}$$

According to Beer-Lambert Law:[52]

$$A_0 = \varepsilon_B L C_0 \tag{16}$$

$$A_B = \varepsilon_B L C_B \tag{17}$$

$$A_F = \varepsilon_F L C_F \tag{18}$$

where $\varepsilon_B$ and $\varepsilon_F$ are the extinction coefficient of the pair-bonded hydroxyl groups and free hydroxyl groups, respectively.

At a given temperature between $T_{low}$ and $T_{high}$, the molar fraction of the pair-bonded hydroxyl groups is:

$$\alpha_B = \frac{C_B}{C_0} = \frac{A_B/\varepsilon_B L}{A_0/\varepsilon_B L} = \frac{A_B}{A_0} \tag{19}$$

The mole fraction of free hydroxyl groups can be expressed as:

$$\alpha_F = \frac{C_F}{C_0} = \frac{C_0 - C_B}{C_0} = 1 - \frac{C_B}{C_0} = 1 - \alpha_B \tag{20}$$

The equilibrium constant of the equation (13) can be calculated from:

$$K = \frac{[H-O\cdots H-O]}{[H-O][H-O]} = \frac{\alpha_B}{(1-\alpha_B)^2 C_0} \tag{21}$$

The equation (21) can be transformed into Van't Hoff form:

$$\ln K = \ln[\frac{\alpha_B}{(1-\alpha_B)^2}] - \ln C_0 = -\frac{\Delta H_h}{R}\cdot\frac{1}{T} + \frac{\Delta S}{R} \tag{22}$$

$$\ln[\frac{\alpha_B}{(1-\alpha_B)^2}] = -\frac{\Delta H_h}{R}\cdot\frac{1}{T} + \frac{\Delta S}{R} + \ln C_0 \tag{23}$$

where T is the absolute temperature in Kelvin. R is the gas constant of 8.314 J/mol·K. $\Delta H_h$ is the enthalpy of pair-bonded hydrogen bonding (J/mol), and ΔS is entropy of pair-bonded hydrogen bonding (J/mol·K).

So a straight line can be fitted from the plot between $\ln[\alpha_B/(1-\alpha_B)^2]$ and 1/T using the least squares fitting. The enthalpy of the pair-bonded hydrogen bonding of hydroxyl groups can be easily obtained from the slope of the fitted line.

Similarly, the crystallization enthalpy of VA (represented by 1139 $cm^{-1}$) and ET repeating unit (represented by 725 $cm^{-1}$) can also be calculated using the similar procedure, which is described in detail in the supporting information.

Van't Hoff plots which are calculated from the temperature-dependent FTIR of EVOH are illustrated in **Figure 5**. Three interesting bands were used to perform the Van't Hoff analysis,

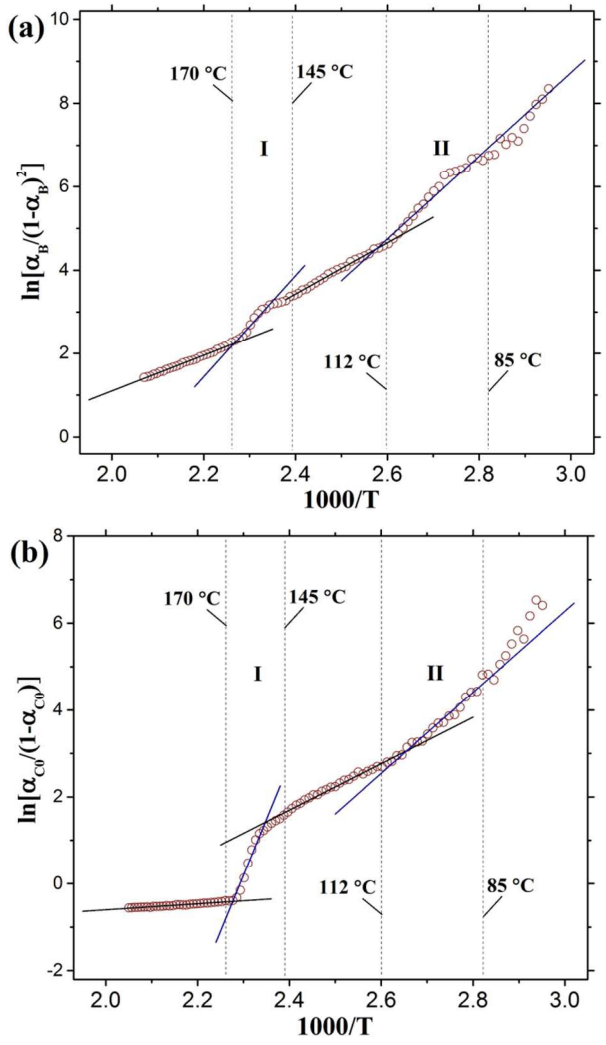

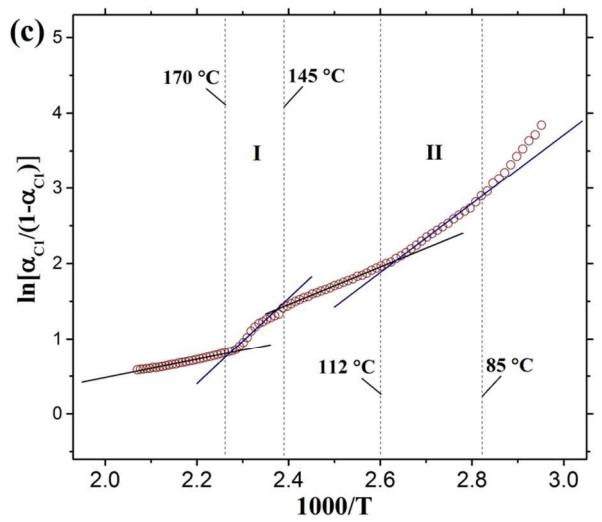


**Figure 5.** Van't Hoff plots from the temperature-dependent FTIR of EVOH. **(a)** Calculating from the absorbance change at 3310 $cm^{-1}$ (the change from 3350 $cm^{-1}$ to 3260 $cm^{-1}$ is actually used), which represents the generation of hydrogen bonds; **(b)** Calculating from the absorbance change at 1139 $cm^{-1}$, which represents the crystallization of VA repeating unit; **(c)** Calculating from the absorbance change at 725 $cm^{-1}$, which represents the crystallization of ET repeating unit.

including the absorbance changes at 3310 $cm^{-1}$, 1139 $cm^{-1}$, and 725 $cm^{-1}$. The reason of choosing these bands is that 3310 $cm^{-1}$ is assigned to hydrogen-bonded O−H groups in VA repeating unit, and 1139 $cm^{-1}$ is attributed to −C−O− groups in VA repeating unit in the crystalline. Moreover, the bands at 725 $cm^{-1}$ is the crystalline characteristic bands of ET repeating unit. That is to say, 3310 $cm^{-1}$ represents the hydrogen bonding of hydroxyl groups in VA repeating unit, and 1139 $cm^{-1}$ and 725 $cm^{-1}$ represent the crystallization of VA repeating unit and ET repeating unit, respectively. Thus, the enthalpy of hydrogen bonds generating and that of the crystallization of EVOH upon cooling can be estimated via Van't Hoff analysis. For obtaining an accurate result, the absorbance change at 3310 $cm^{-1}$ used in **Figure 5** was actually the change from 3350 $cm^{-1}$ to 3260 $cm^{-1}$. This is because the observations of a large drift of the bands from 3350 $cm^{-1}$ to 3260 $cm^{-1}$ in scaling-MW2D FTIR spectra (**Figure 4**). Combining **Figure 4** and **Figure 5**, as shown, two regions of 170−145 °C (region I) and 112−85 °C (region II) can be conveniently determined. According to the discussions of DSC and scaling-MW2D, region I and II are the primary crystallization process and the secondary perfection process, respectively.

In **Figure 5 (a, b, c)**, it can be observed that four straight lines can be successfully fitted for each Van't Hoff plot. This actually indicates the enthalpy splits into 4 regions upon cooling. The estimated enthalpies of these 4 regions are listed in **Table 2**. The minus sign before the number reveals it is an exothermic process. So, a larger absolute value of the enthalpy represents a bigger trend to generate hydrogen bonds or the crystalline. The enthalpy of the pair-bonded hydrogen bonding ($\Delta H_h$) is -32.8±0.3 kJ/mol when the temperature is within 215-172 °C. This temperature is above the primary crystallization (region I), and EVOH is still in the melt state. At the same time, the crystallization enthalpy of VA repeating unit ($\Delta H_{C\text{-}VA}$) is -5.3±0.2 kJ/mol. These reveal that a small amount of hydrogen bonds in EVOH probably still exist at a high temperature. However, the crystallization is impossible due to no impetus at this high temperature. For region I, $\Delta H_h$=-90.4±5.2 kJ/mol and $\Delta H_{C\text{-}VA}$=-170.1±11.8 kJ/mol, a great number of free hydroxyl groups form pair-bonded hydrogen bonds, and a strong crystallization occurs.

It is noted that the absolute value of the calculated enthalpies is different from the usual reported data (10-40 kJ/mol). As mentioned above, the formation of hydrogen bonds involved in EVOH crystallization is pair-bonded, considering the regularity of molecular chains in the crystal

**Table 2.** The enthalpy of the pair-bonded hydrogen bonding and crystallization calculated from Van't Hoff plots in **Figure 5**, and the enthalpy of diffusing into the crystal lattice calculated from equation (24)

| | 215-172 °C | region I | 146-114 °C | region II |
|---|---|---|---|---|
| **Enthalpy of pair-bonded hydrogen bonding of VA repeating unit, $\Delta H_h$ (kJ/mol)** | -32.8±0.3 | -90.4±5.2 | -48.0±0.6 | -75.8±3.1 |
| **Crystallization enthalpy of VA repeating unit, $\Delta H_{C\text{-}VA}$ (kJ/mol)** | -5.3±0.2 | -170.1±11.8 | -42.8±1.2 | -72.6±2.1 |
| **Enthalpy of VA repeating unit diffusing into the crystal lattice, $\Delta H_{I\text{-}VA}$ (kJ/mol)** | -- | -79.7±6.6 | 5.2±0.6 | 3.2±1.0 |
| **Crystallization enthalpy of ET repeating unit, $\Delta H_{C\text{-}ET}$ (kJ/mol)** | -9.4±0.2 | -41.0±2.0 | -20.6±0.2 | -38.3±0.8 |
| **Crystallization enthalpy of entire EVOH (kJ/mol)** | -14.7±0.2 | -211.1±6.9 | -63.4±0.7 | -110.9±1.5 |
| **Contribution of the hydrogen bonding to VA crystallization (%)** | -- | 53.1 | -- | 95.9 |
| **Contribution of the hydrogen bonding to the whole EVOH crystallization (%)** | -- | 42.8 | -- | 64.6 |
| **Contribution of VA repeating unit diffusing into the crystal lattice to the whole EVOH crystallization (%)** | | 37.8 | | 2.7 |
| **Contribution of ET crystallization to the whole EVOH crystallization (%)** | -- | 19.4 | -- | 32.7 |
| **Contribution of VA crystallization to the whole EVOH crystallization (%)** | -- | 80.6 (42.8+37.8) | -- | 67.3 (64.6+2.7) |
| **Total (%)** | -- | 100.0 (42.8+37.8+19.4) | -- | 100.0 (64.6+2.7+32.7) |

lattice. That is to say, a pair of hydroxyl produces two hydrogen bonds. Thus, the estimated enthalpies in our study are actually included the enthalpies of two hydrogen bonds formation in a pair of hydroxyl, and the enthalpy of a single hydrogen bond formation is the half of the calculated value, which is very close to that of the usual reported data.

The estimated enthalpies using Van't Hoff method in our work are close to other literature reports.[53-56] In these literatures, Van't Hoff method was also employed to estimate the enthalpy changes from polymer repeating units, especially the enthalpy of hydrogen bonds.

In the chemical structure of VA repeating unit, the hydroxyl group and the ether bond are directly connected, namely, −C−O−H. In general, scientists believed that hydrogen bonding is the direct driving force of leading to the crystallization of PVA or EVOH.[13-15, 32] That is to say, from the molecular structure, the crystalline of VA repeating unit (reflected by 1139 $cm^{-1}$) certainly contains the stable pair-bonded hydrogen bonds of hydroxyl. The generation of pair-bonded hydrogen bonds is an important part of VA repeating unit crystallization. From the point of view of polymer physics, the polymer crystallization needs the molecular repeating unit to be able to smoothly diffuse into the crystal lattice. Thus, there exists the following relationship:

$$\Delta H_{C\text{-}VA} \approx \Delta H_h + \Delta H_{l\text{-}VA} \quad (24)$$

where $\Delta H_{C\text{-}VA}$ is the enthalpy of VA repeating unit crystallization, and $\Delta H_h$ is the enthalpy of pair-bonded hydrogen bonding of VA repeating unit. $\Delta H_{l\text{-}VA}$ is the enthalpy of VA repeating unit diffusing into the crystal lattice. The detailed deduction of this equation is in the supporting information.

The equation (24) shows that both $\Delta H_h$ and $\Delta H_{l\text{-}VA}$ are essential parts of the crystallization enthalpy of VA repeating unit ($\Delta H_{C\text{-}VA}$). It is noted that equations (24) is only correct and reasonable when the temperature is below or equal to the initial crystallization temperature (onset point). In this study, this initial temperature is 170 °C.

For region I, $\Delta H_{l\text{-}VA}$=-79.7±6.6 kJ/mol shows that VA repeating unit of EVOH have a strong tendency to spontaneously form the crystal lattice under the induction of pair-bonded hydrogen bonding, accompanied by a release of the large heat. After region I, $\Delta H_h$=-48.0±0.6 kJ/mol and $\Delta H_{C\text{-}VA}$=-42.8±1.2 kJ/mol, the capacity of forming pair-bonded hydrogen bonds is obviously reduced when the temperature is within 146-114 °C. The calculated $\Delta H_{l\text{-}VA}$ is 5.2±0.6 kJ/mol, and this indicates VA repeating unit never have a capacity to diffuse into the crystal lattice, also reflecting the loss of the molecular chains' movement at a low temperature. In region II, $\Delta H_h$=-75.8±3.1 kJ/mol and $\Delta H_{C\text{-}VA}$=-72.6±2.1 kJ/mol, a number of pair-bonded hydrogen bonds are generated again from free hydroxyl groups. This is probably because a low temperature is more conducive for the formation of pair-bonded hydrogen bonds from free hydroxyl groups. $\Delta H_{l\text{-}VA}$ is calculated as 3.2±1.0 kJ/mol. For region II, a part of molecular repeating unit gain the local motion ability due to the bonding of pair-bonded hydrogen bonds, resulting in a local rearrangement of the lattice in imperfect crystalline. The VA repeating unit absorb energy of 3.2±1.0 kJ/mol from the enthalpy of pair-bonded hydrogen bonding to obtain this local motion to recrystallize. From the view point of the releasing and absorbing enthalpy, the contribution of the pair-bonded hydrogen bonding to VA crystallization in region I and II can be estimated:

$$Contributi\,on_{h-to-VA} = \frac{|\Delta H_h|}{|\Delta H_h| + |\Delta H_{l-VA}|} \times 100\% \quad (25)$$

As listed in **Table 2**, the contribution of the pair-bonded hydrogen bonding to VA crystallization is 53.1% and 95.9% during the primary (region I) and the secondary perfection process (region II), respectively.

For the whole EVOH, it is important to note that its crystallization is contributed from both the crystallization of ET and VA repeating unit. Thus, the ET crystallization also needs to focus on.

In **Table 2**, it can be seen that the crystallization enthalpy of ET repeating unit ($\Delta H_{C\text{-}ET}$) is -9.4±0.2 kJ/mol when the temperature is above region I (within 215-172 °C). This indicates that the crystallization of ET repeating unit is impossible, which is similar with VA repeating unit ($\Delta H_{C\text{-}VA}$=-5.3±0.2 kJ/mol). As everyone knows, EVOH is in a molten state at such a high temperature, and therefore, the crystallization cannot occur. In region I, $\Delta H_{C\text{-}ET}$ is -41.0±2.0 kJ/mol, and the ET repeating unit crystallization take places. However, the absolute value of $\Delta H_{C\text{-}ET}$ is significantly less than that of VA repeating unit ($\Delta H_{C\text{-}VA}$=-170.1±11.8 kJ/mol), and even obviously less than the enthalpy of pair-bonded hydrogen bonding of VA repeating unit ($\Delta H_h$=-90.4±5.2 kJ/mol). This clearly shows that the crystallization trend of ET repeating unit is much weaker than that of VA repeating unit. Comparing with VA repeating unit, the ET repeating unit crystallization can only be called a weak crystallization. In region II, $\Delta H_{C\text{-}ET}$=-38.3±0.8 kJ/mol, its absolute value is also obviously less than that of $\Delta H_{C\text{-}VA}$ (-72.6±2.1 kJ/mol) and $\Delta H_h$ (-75.8±3.1 kJ/mol). From the viewpoint of thermodynamics, this result still reveals that the crystallization trend of VA repeating unit is much larger than that of ET repeating unit. It is noted that $\Delta H_{C\text{-}ET}$ is -20.6±0.2 kJ/mol when the temperature is within 146-114 °C (below region I and above region II). The absolute value of this value is even lower than that of in region II (-38.3±0.8 kJ/mol), which reveals the enhancement of the crystallization ability of ET repeating unit for some reason in region II. Overall, such as VA repeating unit, the ET crystallization is an indispensable part of the whole EVOH crystallization.

The contribution of the pair-bonded hydrogen bonding, as well as VA repeating unit diffusing into the crystal lattice, to the whole EVOH crystallization can be calculated according to the following equations:

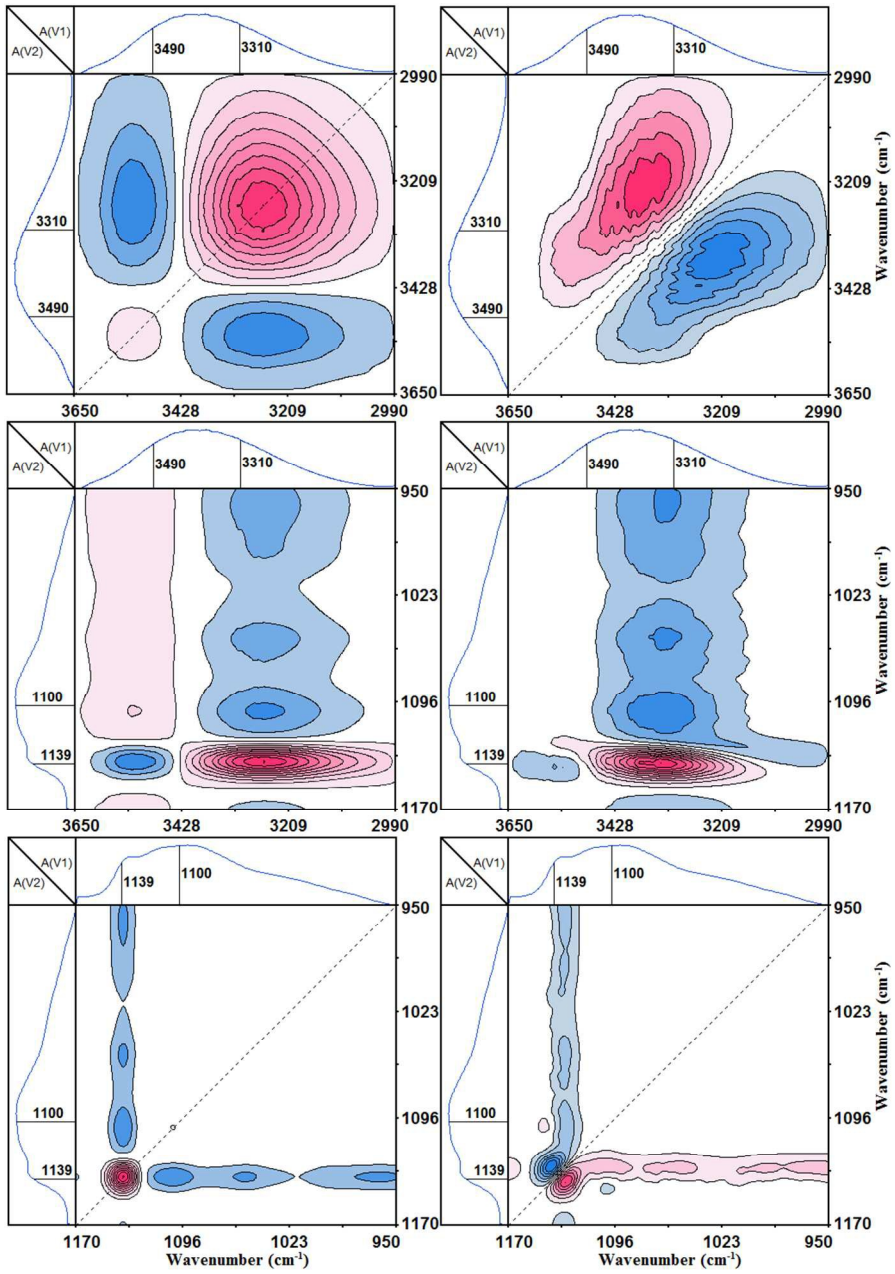


**Figure 6**. Synchronous (left) and asynchronous (right) FTIR spectra calculated from temperature-dependent spectra of region I (170–145 °C) in the region 3650–2990 $cm^{-1}$, 3650–2990 $cm^{-1}$ *vs* 1170–950 $cm^{-1}$, and 1170–950 $cm^{-1}$. Pink and blue areas represent the positive and negative correlation intensity, respectively.

$$Contribution_{h-to-EVOH} = \frac{|\Delta H_h|}{|\Delta H_{C-ET}|+|\Delta H_h|+|\Delta H_{l-VA}|} \times 100\% \quad (26)$$

$$Contribution_{l-to-EVOH} = \frac{|\Delta H_{l-VA}|}{|\Delta H_{C-ET}|+|\Delta H_h|+|\Delta H_{l-VA}|} \times 100\% \quad (27)$$

Here, $\Delta H_{C\text{-}ET}$ is the crystallization enthalpy of ET repeating unit, and $\Delta H_{l\text{-}VA}$ is the enthalpy of VA repeating unit diffusing into the crystal lattice, $\Delta H_h$ represents the enthalpy of pair-bonded hydrogen bonding of VA repeating unit. The detailed deduction of above two equations can refer to the supporting information.

Similarly, the contributions of ET and VA repeating unit crystallization to the whole EVOH crystallization can also be calculated from equations (28) and (29):

$$Contribution_{ET-to-EVOH} = \frac{|\Delta H_{C-ET}|}{|\Delta H_{C-ET}|+|\Delta H_h|+|\Delta H_{l-VA}|} \times 100\% \quad (28)$$

$$Contribution_{VA-to-EVOH} = 100 - Contribution_{ET-to-EVOH} \quad (29)$$

For region I and region II, the contributions of VA crystallization, ET crystallization, and the pair-bonded hydrogen bonding to the whole EVOH crystallization are calculated. As listed in **Table 2**, in region I, the contribution of VA crystallization to the whole EVOH crystallization is 80.6%; however, that of ET repeating unit only reaches to 19.4%. In region II, the contributions of VA and ET crystallization are 67.3% and 32.7%, respectively. These results fully demonstrate that, in both regions I and II, VA crystallization is the majority, and ET crystallization is minority. Thus, EVOH crystallization is dominated by VA repeating unit. In addition, the contributions of the hydrogen bonding to the VA crystallization in region I and region II are 53.1% and 95.9 %, respectively. That is to say, the pair-bonded hydrogen bonding dominates the crystallization of VA repeating unit. So, the important rule of pair-bonded hydrogen bonding on the whole EVOH crystallization is apparent. In **Table 2,** the contributions of the pair-bonded hydrogen bonding to the whole EVOH crystallization in regions I and II are 42.8% and 64.6%, which is obviously higher than that of ET repeating unit (19.4% and 32.7%). The contribution of the pair-bonded hydrogen bonding to the whole EVOH crystallization is approximately twice that of ET repeating unit.

### 3.5. Generalized 2D correlation analysis

To capture a detail mechanism, as well as to understand the role of hydrogen bonding, during the crystallization of EVOH copolymer, the temperature-dependent FTIR spectra within region I (170-145 °C) and II (112-85 °C) were used to perform the generalized 2D correlation analysis. Generalized 2D FTIR spectra contain synchronous and asynchronous spectra. The sequential order of the spectral intensity changing at given wavenumber can be conveniently probed by the sign of the correlation peaks using Noda's rules. A simple summarization of Noda's rules is as follows:[22]

1) If $\Phi(\nu_1, \nu_2)>0$, $\Psi(\nu_1, \nu_2)>0$ or $\Phi(\nu_1, \nu_2)<0$, $\Psi(\nu_1, \nu_2)<0$, then the movement of $\nu_1$ is before that of $\nu_2$;

2) If $\Phi(\nu_1, \nu_2)>0$, $\Psi(\nu_1, \nu_2)<0$ or $\Phi(\nu_1, \nu_2)<0$, $\Psi(\nu_1, \nu_2)>0$, then the movement of $\nu_1$ is after that of $\nu_2$;

3) If $\Phi(\nu_1, \nu_2)>0$, $\Psi(\nu_1, \nu_2)=0$ or $\Phi(\nu_1, \nu_2)<0$, $\Psi(\nu_1, \nu_2)=0$, then the movements of $\nu_1$ and $\nu_2$ are simultaneous.

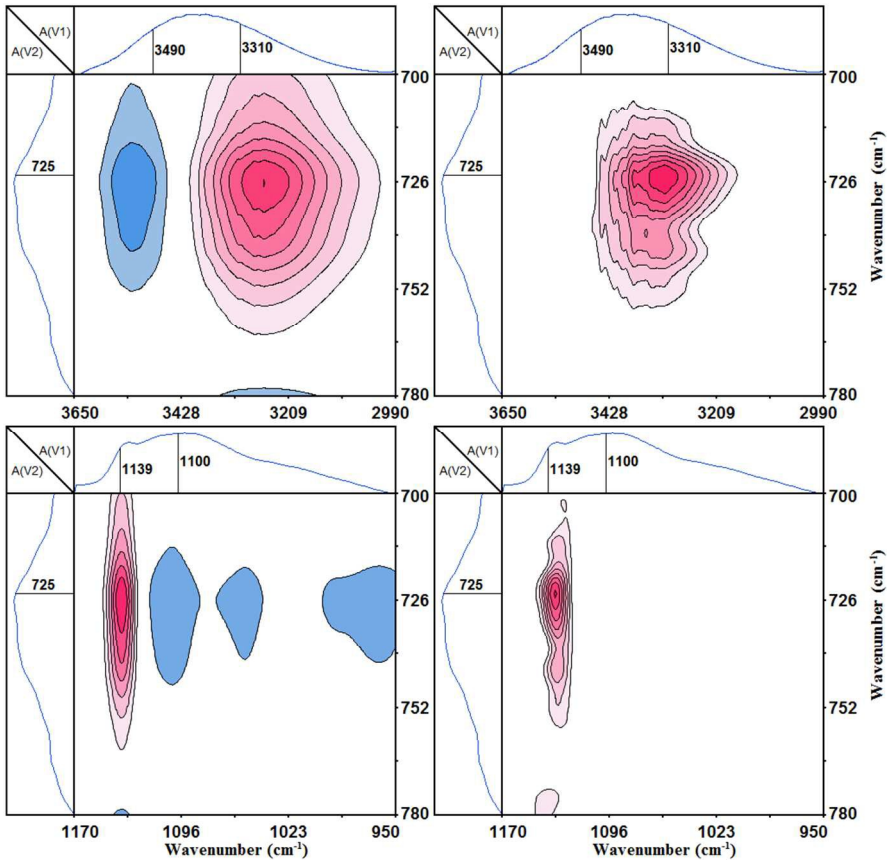


**Figure 7.** Synchronous (left) and asynchronous (right) FTIR spectra calculated from temperature-dependent spectra of region I (170−145 °C) in the region 3650−2990 $cm^{-1}$ *vs* 780−700 $cm^{-1}$ and 1170−950 $cm^{-1}$ *vs* 780−700 $cm^{-1}$.

#### 3.5.1. Region I

##### 3.5.1.1. Sequential order of O−H groups and −C−O− groups in VA repeating unit

The generalized 2D correlation FTIR spectra in the region 3650−2990 $cm^{-1}$, 3650−2990 $cm^{-1}$ *vs* 1170−950 $cm^{-1}$, and 1170−950 $cm^{-1}$ are shown in **Figure 6**, which is calculated from temperature-dependent spectra of region I (170−145 °C).

The left is the synchronous spectra, and the right is the asynchronous spectra. The pink areas and the blue areas represent the positive and the negative correlation intensity, respectively. The signs of the correlation peaks among 3490 $cm^{-1}$, 3310 $cm^{-1}$, 1139 $cm^{-1}$, and 1100 $cm^{-1}$ are summarized in **Table 3**. According to Noda's rules, the sequential order is 3310 $cm^{-1}$→1139 $cm^{-1}$→1100 $cm^{-1}$=3490 $cm^{-1}$. In this study, the symbol "→" represents "before", and "←" represents "after". The corresponding sequential order of groups is $\nu$(O−H, bonded)→$\nu_s$(−C−O−, crystals)→$\nu_s$(−C−O−, amorphous)=$\nu$(O−H, free). This clearly shows that the first step of the primary crystallization of VA repeating unit is the formation of hydrogen bonds, and then the second step of VA repeating unit diffusing into the crystal lattice is followed, resulting in VA repeating unit crystallization. The third step is the movement of VA repeating unit with no hydrogen bonds in amorphous. The sequential order gained from 2D correlation analysis is fully consistent with scientists' previous assumption that the crystallization of EVOH was induced via the hydrogen bonding.[13-15, 32] As listed in **Table 2**, the estimated enthalpy of the pair-bonded hydrogen bonding $\Delta H_h$ is -90.4±5.2 kJ/mol, and the contribution of the pair-bonded hydrogen bonding to VA repeating unit crystallization is calculated as 53.1% within region I. All of these data reveal the important role of the hydrogen bonding on the primary crystallization of EVOH. Without the pair-bonded hydrogen bonding, the molecular chains of VA repeating unit in EVOH will have no ability to smoothly diffuse into the crystal lattice and to maintain the stability of the lattice.

**Table 3.** Sequential orders of the bands of O−H groups, −C−O− groups in VA repeating unit, and $-CH_2-$ groups in ET repeating unit gained from **Figure 6** and **Figure 7**.

| Cross correlation peak ($cm^{-1}$) | Sign in synchronous spectra | Sign in asynchronous spectra | Sequential order |
|---|---|---|---|
| (3490, 3310) | - | + | 3490←3310 |
| (3490, 1100) | + | 0 | 3490=1100 |
| (3490, 1139) | - | + | 3490←1139 |
| (3310, 1100) | - | - | 3310→1100 |
| (3310, 1139) | + | + | 3310→1139 |
| (1139, 1100) | - | - | 1139→1100 |
| 3310 $cm^{-1}$→1139 $cm^{-1}$→1100 $cm^{-1}$=3490 $cm^{-1}$ | | | |
| (3490, 725) | - | 0 | 3490=725 |
| (3310, 725) | + | + | 3310→725 |
| (1139, 725) | + | + | 1139→725 |
| (1100, 725) | - | 0 | 1100=725 |
| 3310 $cm^{-1}$→1139 $cm^{-1}$→1100 $cm^{-1}$=3490 $cm^{-1}$=725 $cm^{-1}$ | | | |
| $\nu$(O−H, bonded)→$\nu_s$(−C−O−, crystals)→$\nu_s$(−C−O−, amorphous)=$\nu$(O−H, free)=$\gamma$($-CH_2-$, crystals) | | | |

### 3.5.1.2. Sequential order of O−H groups,−C−O− groups in VA repeating unit, and $-CH_2-$ groups in ET repeating unit

EVOH contains both VA and ET repeating unit. Thus, the sequential order among the representative groups of VA and ET repeating unit was also studied by 2D correlation analysis. **Figure 7** illustrates the generalized 2D correlation FTIR spectra in the region 3650−2990 $cm^{-1}$ *vs* 780−700 $cm^{-1}$ and 1170−950 $cm^{-1}$ *vs* 780−700 $cm^{-1}$. The signs of the studied correlation peaks are also summarized in **Table 3**. The complete sequential order is 3310 $cm^{-1}$→1139 $cm^{-1}$→1100 $cm^{-1}$=3490 $cm^{-1}$=725 $cm^{-1}$, namely, $\nu$(O−H, bonded)→$\nu_s$(−C−O−, crystals)→$\nu_s$(−C−O−, amorphous)=$\nu$(O−H, free)=$\gamma$($-CH_2-$, crystals). Region I is a 3-steps process. The results of 2D correlation analysis reveal that the generation of the hydrogen bonds in VA repeating unit is the key step of the primary crystallization of EVOH (159 °C). It is inferred that the movements between $-CH_2-$ groups in ET repeating unit and −C−O−H groups in VA repeating unit with no hydrogen bonds are simultaneous, which also indicates the time of ET repeating unit crystallization is the same as that of VA repeating unit in amorphous. It can also be understood that the formation of ET repeating unit crystalline is accompanied by the movement of VA repeating unit without hydrogen bonding in the amorphous within region I.

**Table 4.** Sequential orders of the bands of O−H groups, −C−O− groups in VA repeating unit, and $-CH_2-$ groups in ET repeating unit gained from **Figure 8** and **Figure 9**.

| Cross correlation peak ($cm^{-1}$) | Sign in synchronous spectra | Sign in asynchronous spectra | Sequential order |
|---|---|---|---|
| (3490, 3310) | - | + | 3490←3310 |
| (3490, 1100) | + | 0 | 3490=1100 |
| (3490, 1139) | - | + | 3490←1139 |
| (3310, 1100) | - | - | 3310→1100 |
| (3310, 1139) | + | + | 3310→1139 |
| (1139, 1100) | - | - | 1139→1100 |
| 3310 $cm^{-1}$→1139 $cm^{-1}$→3490 $cm^{-1}$=1100 $cm^{-1}$ | | | |
| (3490, 725) | - | - | 3490→725 |
| (3310, 725) | + | + | 3310→725 |
| (1139, 725) | + | + | 1139→725 |
| (1100, 725) | - | - | 1100→725 |
| 3310 $cm^{-1}$→1139 $cm^{-1}$→3490 $cm^{-1}$=1100 $cm^{-1}$→725 $cm^{-1}$ | | | |
| $\nu$(O−H, bonded)→$\nu_s$(−C−O−, crystals)→$\nu_s$(−C−O−, amorphous)=$\nu$(O−H, free)→$\gamma$($-CH_2-$, crystals) | | | |

### 3.5.2. Region II

### 3.5.2.1. Sequential order of O−H groups and −C−O− groups in VA repeating unit

**Figure 8** are the generalized 2D correlation FTIR spectra calculated from temperature-dependent spectra of region II (112−85 °C) in the region 3650−2990 $cm^{-1}$, 3650−2990 $cm^{-1}$ *vs* 1170−950 $cm^{-1}$, and 1170−950 $cm^{-1}$. The signs of the correlation peaks are summarized in **Table 4**. The sequential order is 3310 $cm^{-1}$→1139 $cm^{-1}$→1100 $cm^{-1}$=3490 $cm^{-1}$, namely, $\nu$(O−H, bonded)→$\nu_s$(−C−O−, crystals)→$\nu_s$(−C−O−, amorphous)=$\nu$(O−H, free). This sequential order of region II is completely identical with that gained in region I. The first step of the secondary perfection process of VA repeating unit is also the generation of hydrogen bonds. As listed in **Table 2**, the contribution of the pair-bonded hydrogen bonding to VA repeating unit crystallization is 95.9% in region II, and the enthalpy of the pair-bonded hydrogen bonding $\Delta H_h$ is -75.8±3.1 kJ/mol. The difference (of the second step in region II) from the region I is that this is a local rearrangement of the

lattice in imperfect crystalline, called as secondary perfection process. The third step is the movement of VA repeating unit with no hydrogen bonds in the amorphous, which is also the same as the inferred from region I. These results disclose that the hydrogen bonding plays a leading role on the secondary perfection process of EVOH, which is more important than region I.

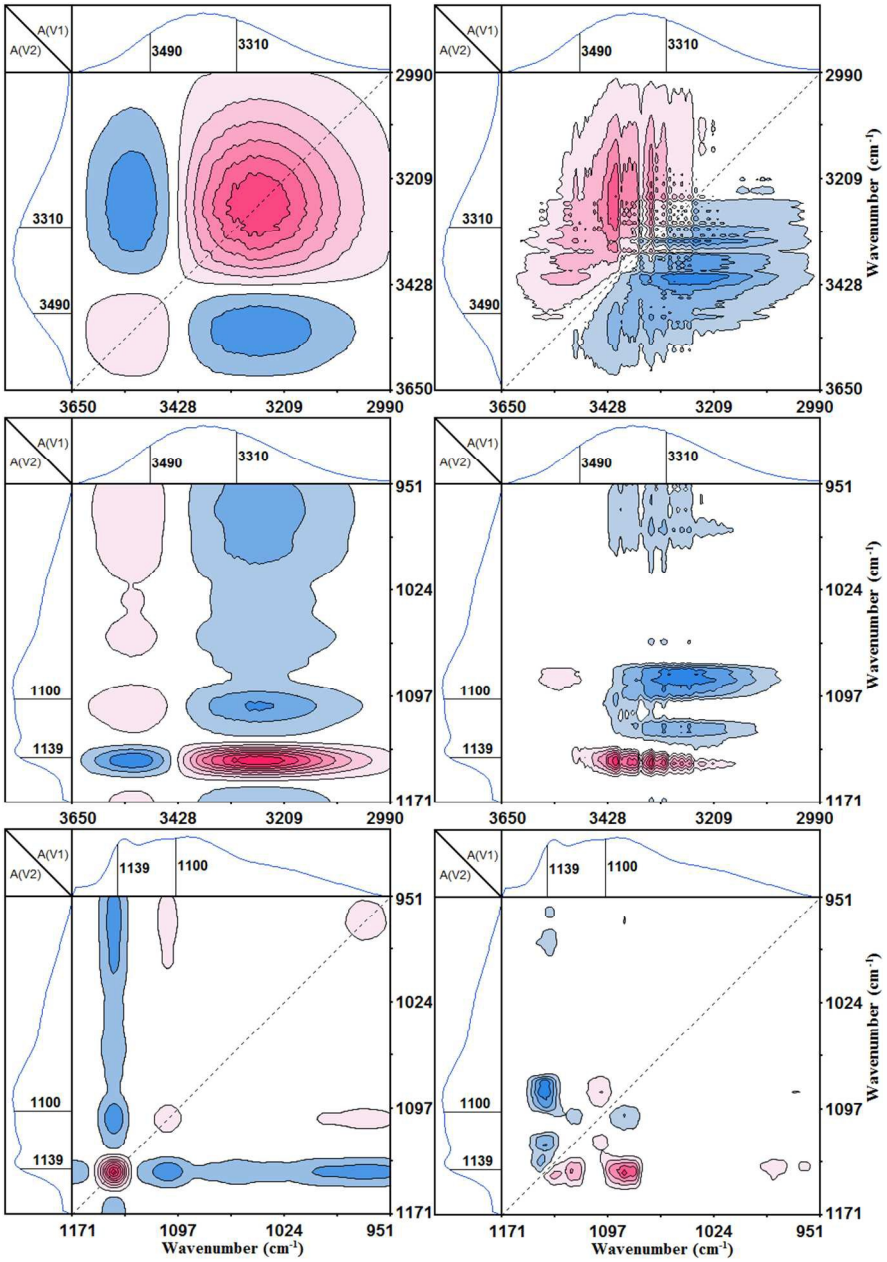


**Figure 8.** Synchronous (left) and asynchronous (right) FTIR spectra calculated from temperature-dependent spectra of region II (112–85 °C) in the region 3650–2990 $cm^{-1}$, 3650–2990 $cm^{-1}$ *vs* 1170–950 $cm^{-1}$, and 1170–950 $cm^{-1}$. Pink and blue areas represent the positive and negative correlation intensity, respectively.

### 3.5.2.2. Sequential order of O−H groups, −C−O− groups in VA repeating unit, and $-CH_2-$ groups in ET repeating unit

**Figure 9** illustrates the generalized 2D correlation FTIR spectra in the region 3650−2990 $cm^{-1}$ *vs* 780−700 $cm^{-1}$ and 1170−950 $cm^{-1}$ *vs* 780−700 $cm^{-1}$. The signs of the correlation peaks are also summarized in **Table 4**. The complete sequential order is 3310 $cm^{-1}$→1139 $cm^{-1}$→3490 $cm^{-1}$=1100 $cm^{-1}$→725 $cm^{-1}$. The corresponding movements of groups is $\nu$(O−H, bonded)→$\nu_s$(−C−O−, crystals)→$\nu_s$(−C−O−, amorphous)=$\nu$(O−H, free)→$\gamma(-CH_2-$, crystals). Obviously, the $-CH_2-$ of ET repeating unit is the last groups to move within region II, which also indicates that the secondary perfection process of ET repeating unit is after that of VA repeating unit. The sequential order of $-CH_2-$ groups of ET repeating unit is different from the findings in region I. This reveals the occurrence of a sub-process after the movement of

VA repeating unit. Thus, region II is a 4-steps process. The fourth step is probably due to the weak crystallization of ET repeating unit at a low temperature. We can also gain that the movement of ET repeating unit is a forced movement dominated by VA repeating unit.

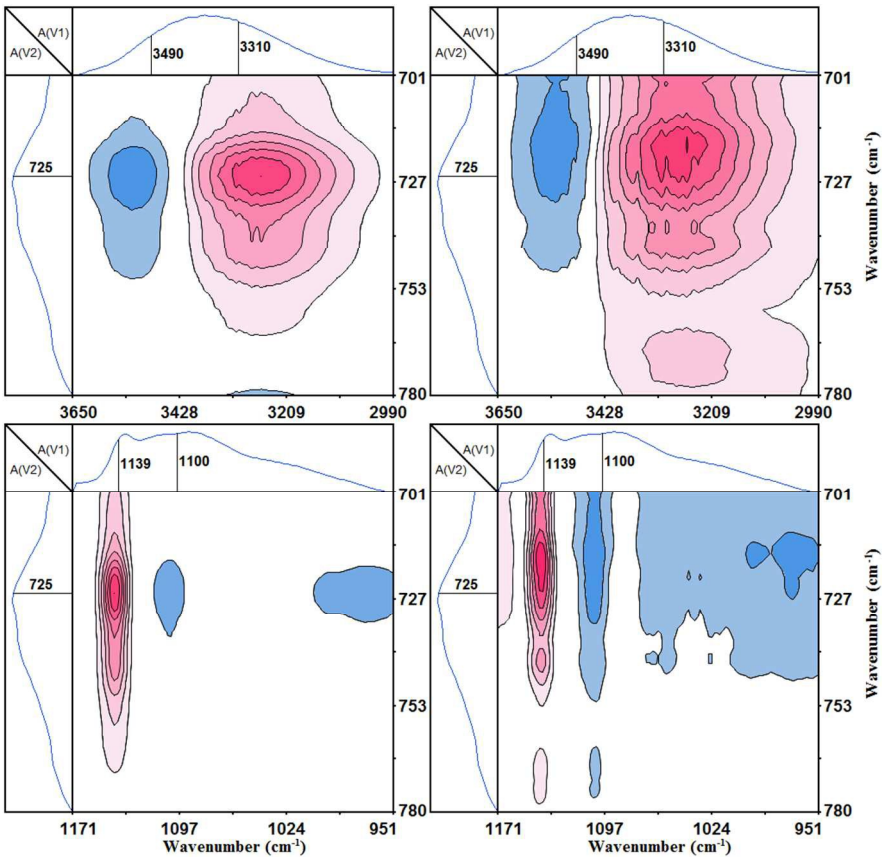


**Figure 9**. Synchronous (left) and asynchronous (right) FTIR spectra calculated from temperature-dependent spectra of region II (112−85 °C) in the region 3650−2990 $cm^{-1}$ *vs* 780−700 $cm^{-1}$ and 1170−950 $cm^{-1}$ *vs* 780−700 $cm^{-1}$.

## 4. Conclusions

In this study, two regions of EVOH crystallization were detected via the combination of DSC curves and the newly proposed scaling-MW2D correlation FTIR spectroscopy. The region I is the primary crystallization with the maximum crystallization temperature at 159 °C, and the region II is the secondary perfection process around 101-105 °C. Compared with the conventional MW2D, scaling-MW2D successfully distinguished region II, which was a very weak transition of EVOH.

The detailed steps of region I and region II inferred from the 2D correlation analysis are illustrated in **Scheme 1**. Region I is the primary crystallization of EVOH, which undergoes 3 steps. Region II is the secondary perfection process, which has 4 steps. In **Scheme 1**, the red balls represent VA repeating unit of EVOH, and the black balls represent ET repeating unit. The crystalline of EVOH is represented by light blue areas, and gray areas are the amorphous. For region I (170−145 °C), the first step is the formation of pair-bonded hydrogen bonds ($\Delta H_h$=-90.4±5.2 kJ/mol) in VA repeating unit. The second step is VA repeating unit spontaneously diffusing into the lattice to crystallize ($\Delta H_{l\text{-}VA}$=-79.7±6.6 kJ/mol). This step is induced by the first step (pair-bonded hydrogen bonding). The third step is the ET repeating unit crystallization ($\Delta H_{C\text{-}ET}$=-41.0±2.0 kJ/mol) accompanied by the movement of VA repeating unit without hydrogen bonding in the amorphous. After the temperature decreases to region II (112−85 °C), the secondary perfection process of EVOH occurs. The first step of region II is the generation of pair-bonded hydrogen bonds ($\Delta H_h$=-75.8±3.1 kJ/mol) of VA repeating unit from residual free hydroxyl groups after region I, and the second step is the local rearrangement of the lattice in imperfect crystalline of VA repeating unit. It is noticed that the value of $\Delta H_{l\text{-}VA}$ in this step is 3.2±1.0 kJ/mol, which shows the rearrangement needs to absorb heat. The pair-bonded hydrogen bonding just releases of an amount of the enthalpy for absorption. Thus, the second step of region II in also induced by the first step. The third step of region II is the movement of VA repeating unit with no hydrogen bonds (possibly a local rotation). The fourth step is a weak crystallization of ET repeating unit ($\Delta H_{C\text{-}ET}$=-38.3±0.8 kJ/mol), which probably caused by the movement of VA repeating unit direct connecting with ET repeating unit in the third step. From the view point of the enthalpy, for region I



 

and II, the contributions of the pair-bonded hydrogen bonding to EVOH crystallization are calculated as 42.8% and 64.6%, respectively. At the same time, the contributions of the ET repeating unit crystallization to EVOH crystallization are 19.4% and 32.7%, respectively.

In the present study, the leading role of the hydrogen bonding on the primary and secondary perfection process of EVOH was elucidated and confirmed from a quantitative way and the molecular movements.

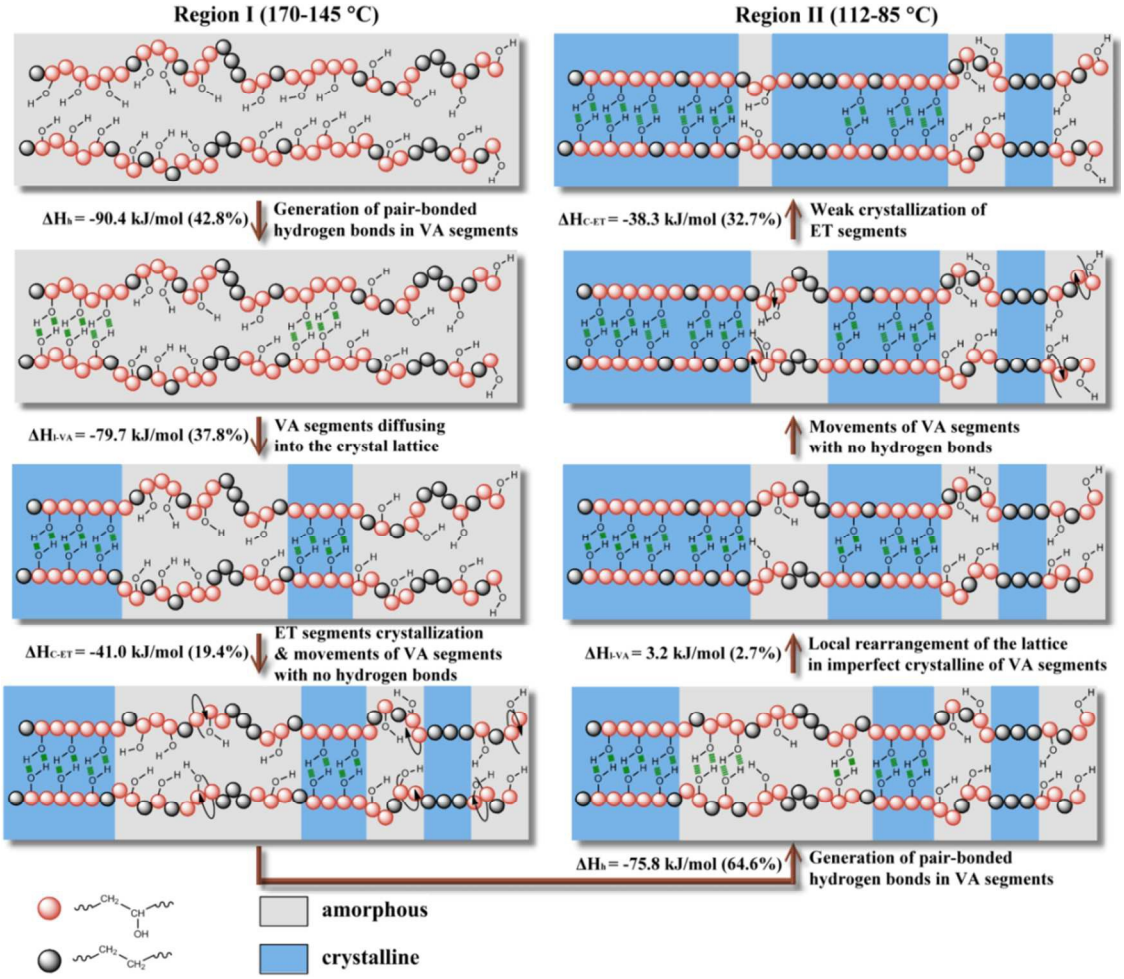


**Scheme 1.** The detailed steps of region I and region II inferred from the 2D correlation analysis. Region I is the primary crystallization of EVOH, which undergoes 3 steps. Region II is the secondary perfection process, which has 4 steps. The red balls represent VA repeating unit of EVOH, and the black balls represent ET repeating unit. The crystalline of EVOH is represented by light blue areas, and gray areas are the amorphous.

## Acknowledgements

This work was supported by the National Natural Science Foundation of China (Grant Nos. 51473104, 51003066), State Key Laboratory of Polymer Materials Engineering (Grant No. sklpme2014-3-06), and the Outstanding Young Scholars Foundation of Sichuan University (Grant No. 2011SCU04A13).

## Notes and references

[a] State Key Laboratory of Polymer Materials Engineering of China, Polymer Research Institute, Sichuan University, Chengdu 610065, China

*Corresponding author. Tel.: +86-28-85402601; Fax: +86-28-85402465; E-mail address: zhoutaopoly@scu.edu.cn (T. Zhou); jjbao2000@sina.com (J. Bao)

1. T. Cornitius, *Chem. Week*, 1997, **159**, 32-32.
2. M. C. Gabriele, *Modern Plastics*, 1997, **74**, 42.
3. K. Ito, Y. Saito, T. Yamamoto, Y. Ujihira and K. Nomura, *Macromolecules*, 2001, **34**, 6153-6155.
4. A. Nakano, in *High-Performance Membrane Dialyzers*, eds. A. Saito, H. Kawanishi, A. C. Yamashita and M. Mineshima, 2011, vol. 173, pp. 164-171.
5. J. H. Schut, *Plastics World*, 1997, **55**, 12-12.
6. A. Lopez-Rubio, J. M. Lagaron, E. Gimenez, D. Cava, P. Hernandez-Munoz, T. Yamamoto and R. Gavara, *Macromolecules*, 2003, **36**, 9467-9476.

7. O. A. Scherman, R. Walker and R. H. Grubbs, *Macromolecules*, 2005, **38**, 9009-9014.
8. J. M. Lagaron, A. K. Powell and G. Bonner, *Polym. Test.*, 2001, **20**, 569-577.
9. T.-H. Young, J.-Y. Lai, W.-M. You and L.-P. Cheng, *J. Membr. Sci.*, 1997, **128**, 55-65.
10. G. D. Guerra, N. Barbani, L. Lazzeri, L. Lelli, M. Palla and C. Rizzo, *J. Biomat. Sci., Polym. E.*, 1993, **4**, 643-652.
11. D. Dorman, E. Otocka and F. Bovey, *Macromolecules*, 1972, **5**, 574-577.
12. R. Foster, *Modern Plastics. Mid-October Encyclopedia Issue,* McGraw-Hill: New York, 1990, **67**, 73.
13. M. Takahashi, K. Tashiro and S. Amiya, *Macromolecules*, 1999, **32**, 5860-5871.
14. K. Nakamae, M. Kameyama and T. Matsumoto, *Polym. Eng. Sci.*, 1979, **19**, 572-578.
15. M. L. Cerrada, E. Pérez, J. M. Pereña and R. Benavente, *Macromolecules*, 1998, **31**, 2559-2564.
16. A. Lopez-Rubio, J. M. Lagaron, E. Gimenez, D. Cava, P. Hernandez-Muñoz, T. Yamamoto and R. Gavara, *Macromolecules*, 2003, **36**, 9467-9476.
17. T. Iwanami and Y. Hirai, *Tappi J.*, 1983, **66**, 85-90.
18. Z. Peter, C. Kenyo, K. Renner, C. Krohnke and B. Pukanszky, *Express Polym. Lett.*, 2014, **8**, 756-766.
19. C. Lopez-de-Dicastillo, J. M. Alonso, R. Catala, R. Gavara and P. Hernandez-Munoz, *J. Agric. Food Chem.*, 2010, **58**, 10958-10964.
20. S. Dhawan, C. Varney, G. V. Barbosa-Canovas, J. M. Tang, F. Selim and S. S. Sablani, *J. Food Eng.*, 2014, **128**, 40-45.
21. S. Aucejo, R. Catala and R. Gavara, *Food Sci. Technol. Int.*, 2000, **6**, 159-164.
22. I. Noda, *Appl. Spectrosc.*, 1993, **47**, 1329-1336.
23. I. Noda and Y. Ozaki, in *Two-Dimensional Correlation Spectroscopy – Applications in Vibrational and Optical Spectroscopy*, John Wiley & Sons, Ltd, 2005.
24. M. Thomas and H. H. Richardson, *Vib. Spectrosc*, 2000, **24**, 137-146.
25. S. Morita, H. Shinzawa, I. Noda and Y. Ozaki, *Appl. Spectrosc.*, 2006, **60**, 398-406.
26. T. Zhou, Y. Liu, L. Peng, Y. Zhan, F. Liu, A. Zhang and L. Li, *Anal. Bioanal. Chem.*, 2014, 1-16.
27. W. Li, B. Sun and P. Wu, *Carbohydr. Polym.*, 2009, **78**, 454-461.
28. B. Zhang, H. Tang and P. Wu, *Polym. Chem.*, 2014, **5**, 5967-5977.
29. H. Lai and P. Wu, *Polym. Chem.*, 2013, **4**, 3323-3332.
30. W. Li and P. Wu, *Polym. Chem.*, 2014, **5**, 5578-5590.
31. S. Sun and P. Wu, *Macromolecules*, 2012, **46**, 236-246.
32. L. Peng, T. Zhou, Y. Huang, L. Jiang and Y. Dan, *J. Phys. Chem. B*, 2014, **118**, 9496-9506.
33. B. Sun, Y. Lin, P. Wu and H. W. Siesler, *Macromolecules*, 2008, **41**, 1512-1520.
34. B. Tang, P. Wu and H. Siesler, *J. Phys. Chem. B*, 2008, **112**, 2880-2887.
35. B. Zhang, H. Tang and P. Wu, *Macromolecules*, 2014, **47**, 4728-4737.
36. L. Hou, K. Ma, Z. An and P. Wu, *Macromolecules*, 2014, **47**, 1144-1154.
37. Y. Jing, H. Tang and P. Wu, *Polym. Chem.*, 2013, **4**, 5768-5775.
38. Y. Jin, W. Wang and Z. Su, *Polym. Chem.*, 2012, **3**, 2430-2435.
39. T. Zhou, L. Peng, Y. Liu, Y. Zhan, F. Liu and A. Zhang, *Vib. Spectrosc*, 2014, **70**, 137-161.
40. J. Luo, T. Zhou, X. Fu, H. Liang and A. Zhang, *Eur. Polym. J.*, 2011, **47**, 230-237.
41. Z. Chen, T. Zhou, J. Hui, L. Li, Y. Li, A. Zhang and T. Yuan, *Vib. Spectrosc*, 2012, **62**, 299-309.
42. T. Zhou, Z. Wu, Y. Li, J. Luo, Z. Chen, J. Xia, H. Liang and A. Zhang, *Polymer*, 2010, **51**, 4249-4258.
43. T. Zhou, A. Zhang, C. S. Zhao, H. W. Liang, Z. Y. Wu and J. K. Xia, *Macromolecules*, 2007, **40**, 9009-9017.
44. L. P. Kuhn, *J. Am. Chem. Soc.*, 1952, **74**, 2492-2499.
45. S. Krimm, *Adv. Polym. Sci.*, 1960, **2**, 51-172.
46. J. M. Lagaron, E. Gimenez, R. Catala and R. Gavara, *Macromol. Chem. Phys.*, 2003, **204**, 704-713.
47. H. S. Mansur, C. M. Sadahira, A. N. Souza and A. A. P. Mansur, *Mat. Sci. Eng. C Mater.*, 2008, **28**, 539-548.
48. K. Sugiura, M. Hashimoto, S. Matsuzawa and K. Yamaura, *J. Appl. Polym. Sci.*, 2001, **82**, 1291-1298.
49. L. Dai and L. Ying, *Macromol. Mater. Eng.*, 2002, **287**, 509-514.
50. N. A. Peppas, *Die Makromolekulare Chemie*, 1977, **178**, 595-601.
51. J. M. Gohil, A. Bhattacharya and P. Ray, *J. Polym. Res.*, 2006, **13**, 161-169.
52. D. Swinehart, *J. Chem. Educ.*, 1962, **39**, 333.
53. P. Yang, X. Wang, H. Fan and Y. Gu, *Phys. Chem. Chem. Phys.,* 2013, **15**, 15333-15338.
54. G. A. Senich and W. J. MacKnight, *Macromolecules,* 1980, **13***,* 106-110.
55. L. S. Teo, C. Y. Chen and J. F. Kuo, *Macromolecules,* 1997, **30***,* 1793-1799
56. Q. Yuan, T. Zhou, L. Li, J. Zhang, X. Liu, X. Ke and A. Zhang, *RSC Adv.*, 2015, **5**, 31153-31165.



 